ANALYSIS OF THE ENERGY PERFORMANCE OF A BIOCLIMATIC CERAMIC ENVELOPE

J. Boix [1], G. Silva[1], V. Cantavella[1], F. J. Mira[1], J. E. Juliá[2]

[1] Instituto de Tecnología Cerámica (ITC). Asociación de Investigación de las Industrias Cerámicas (AICE)
Universitat Jaume I. Castellón. Spain.
[2] Departament d'Enginyeria Mecànica i Construcció. Universitat Jaume I. Castellón. Spain.

ABSTRACT

This paper analyses the thermal behaviour of passively functioning ventilated ceramic envelopes used to improve energy performance in buildings. The first part of the study presents a prototype that reproduces irradiation conditions like those found in actual weather conditions in the laboratory, which allows the influence that ceramic tile surface properties have on the tile's capacity to absorb radiant energy to be studied. The paper then describes an experimental module that was built to allow the energy performance of ventilated facades under actual exposure conditions to be studied. The second part of the study sets out a dynamic mathematical model that allows the thermal performance of ventilated facades to be evaluated. The model is validated using the experimental data obtained in the developed prototype.

1. INTRODUCTION

Nowadays, large-sized ceramic tiles are positioning themselves as a singular alternative in the architectural applications market for outdoor envelopes thanks both to their attractiveness and to their optimum performance features, given that they withstand external agents, are practically maintenance-free, and afford high sound and thermal insulation. It is precisely this last point that has the greatest relevance in today's current energy situation, both from the point of view of sustainable development (Kyoto protocol, reduction of energy consumption, public awareness) and of the growing regulatory pressure on building quality (Technical Building Code, EC Directive 2002/91/CE on the Energy Performance of Buildings, Royal Decree 47/2007 on the Energy Certification of Buildings) [1].

Ventilated ceramic envelopes are characterised by having three clearly differentiated areas or sectors: a heat capture sector, a heat transfer channel (HTC), and a stabilisation sector. The heat capture sector is made up of elements designed to absorb the solar radiation impinging on the envelope. The heat transfer channel is the duct behind the capture sector through which the trapped air, fed in through an aperture at the bottom of the envelope, rises as a result of free convection. The stabilisation sector, situated behind the HTC, is generally formed by a wall of high thermal mass which, apart from having a structural function, smoothes the temperature fluctuations that develop throughout the day at the inner face of the envelope. Sometimes the HTC may include insulation in order to maximise heat transfer towards the air circulating on the inside and minimise heat flow through the stabilisation sector.

Although the new requirements for energy performance laid down in the Technical Building Code (HE Basic Document - Energy Saving) will involve an improvement on traditional building systems, the evaluation criteria defined in the document are insufficiently developed with regard to passive ventilation systems, since they merely take heat transfer by conduction through the stabilisation sector into account, removing from the equation the contribution of the remaining elements in the ventilated system and replacing them with the equivalent to an external surface resistance equal to the inner surface resistance of the enclosure. This simplified evaluation criterion is inappropriate for ventilated envelopes, because it fails to take into consideration the thermal effects deriving from the generation of convection streams and other factors that may be relevant for determining energy performance, such as energy transfer by radiation in the HTC or the presence of heat bridges, among others.

The extensive literature available on architectural systems used in sustainable building demonstrates the advantages of natural convection systems as energy-efficient features [2][3][4][5][6]. However, no specific studies have been found that provide scientific information on the thermal behaviour of ventilated ceramic envelopes. Thus, in order to quantify the energy performance of these building systems and assess their possible optimisation, a prototype has been designed in this study to enable the behaviour of ventilated ceramic envelopes under actual exposure conditions to be studied. The experimental data obtained have been used to develop a mathematical model of the thermal performance of ventilated ceramic envelopes.

2. DESIGN OF PROTOTYPES AND EXPERIMENTAL STUDY

2.1. DESIGN OF A SYSTEM THAT REPRODUCES IRRADIATION CONDITIONS

With a view to building an experimental module of a ventilated ceramic envelope in which the capture sector has an optimised radiant energy capturing capacity with respect to currently built envelopes, a study was undertaken to determine how ceramic tile surface properties influence the tile's capacity to absorb impinging solar radiation. For this purpose, a prototype was developed, capable of reproducing irradiation conditions in the laboratory similar to those occurring in actual weather conditions. Tiles with different surface finishes were tested, applying the design of experiments methodology, and the effect of the different finishes on tile radiant-energy absorption capacity was quantified.

2.1.1. Description of the prototype

Figure 1 schematically illustrates the system used to reproduce irradiation conditions. The assembly consists of a 500 W halogen lamp (1) on a 0.5 m long articulated arm (7) which allows the light radiation angle, with respect to the normal to the irradiated surface (θ), to be varied from 0º (radiation normal to the surface) to 90º (radiation horizontal to the surface). It was possible to set the θ angle precisely thanks to an engraved scale (6) on the articulated arm holder.

The test tile (4) rested on the base (2) made of nylon with low heat conductivity, covered with low density insulation (5) to minimise heat losses from the tile towards the assembly. A T-type contact thermocouple (8) was placed in the exact centre on the bottom of the tile; this recorded the tile temperature under different irradiation conditions. The experimental assembly included a longitudinal fan, so that a current of air could be generated (when required) parallel to the surface of the test tiles to simulate the effect of wind on radiation capture.

The tests consisted of determining the maximum temperature reached by the tiles whose surface characteristics were to be evaluated at four different angles of incidence. The test angles were 75.5º, 60º, 41º, and 0º, which correspond to cosθ values of 0.25, 0.5, 0.75, and 1, respectively.

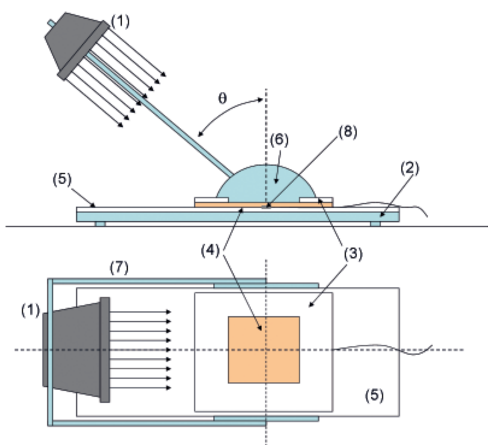

Figure 1. Schematic illustration of the assembly used to reproduce solar irradiation conditions on a laboratory scale.

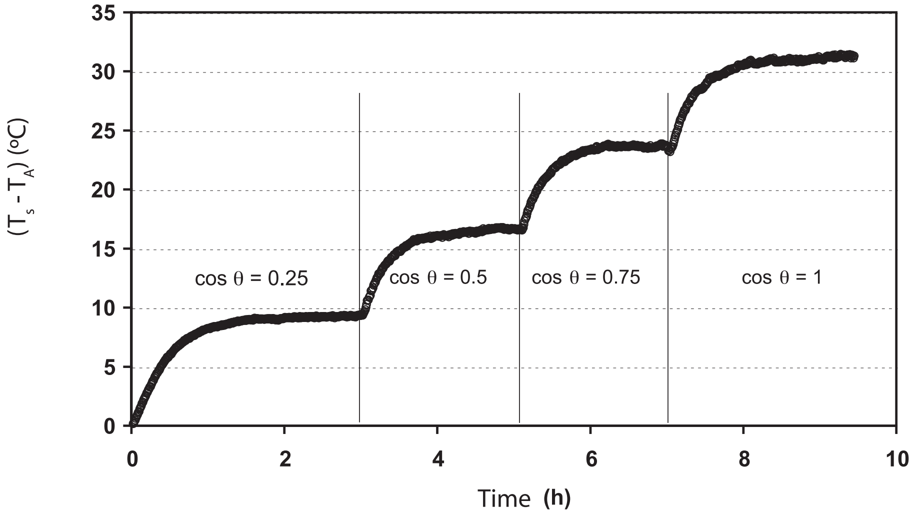

Figure 2. Evolution of the difference between tile temperature and ambient temperature with time.

A graph like the one shown in Figure 2 was obtained for each studied tile, in which the evolution with time of the difference between test piece temperature (T_S) and ambient temperature (T_A), recorded with a T-type thermocouple, is plotted. It may be observed that there was a progressive increase in tile temperature at each test angle, until the temperature stabilised at a maximum value once the steady state was reached.

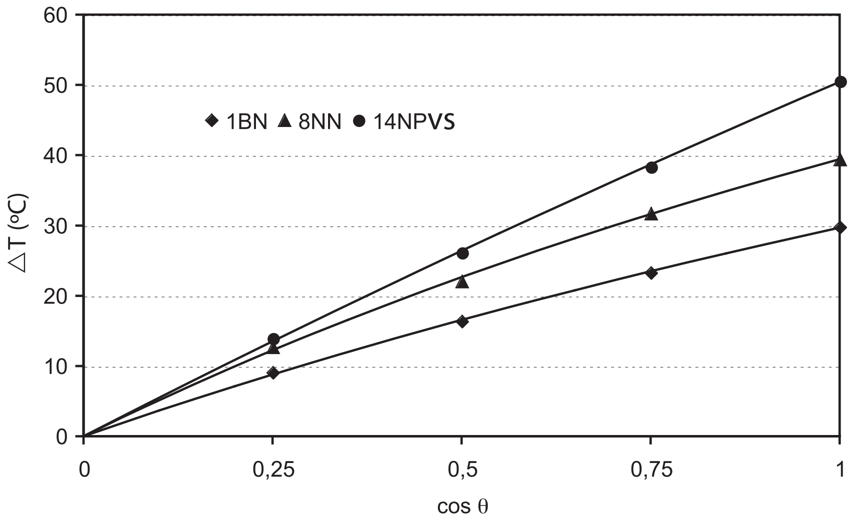

Figure 3. Evolution of the difference between tile temperature and ambient temperature in the steady state with the cosine of the radiation impingement angle.

2.2. ANALYSIS OF VARIABLES

The factors studied with the prototype were as follows:

- Tile colour
- Tile finish
- Existence of a glass on the tiles

- Existence of an air cavity between the tiles and the glass
- Existence of a faceted surface on the tiles
- Presence of wind

In order to analyse the effect of these factors, fourteen 20x20 cm porcelain tiles were prepared with the characteristics shown in Table 1.

Each tile was tested in the developed prototype and a curve was obtained like those for tiles 1, 8, and 14 in Figure 3. These graphs show how the difference in temperature evolved between the tile and the ambient in the steady state as the angle of radiation impingement was modified. The parameter used to quantify the effect of the variables studied on tile absorption capacity was the difference in maximum temperature (ΔT_{max}) reached by the tile during the test. Table 1 presents the values of these parameters for all tested tiles.

Reference	Colour	Surface	Colour (X_1)	Finish (X_2)	Glass (X_3)	Chamber (X_4)	Faceted (X_5)	ΔT_{max} (ºC)
1 BN	White	Rough	0	1	0	0	0	29,8
2 BNV	White	Rough + glass	0	1	1	0	0	38,9
3 BNCV	White	Rough + Chamber + Glass	0	1	1	1	0	38,8
4 BNF	White	Rough + Faceted	0	1	0	0	1	30,6
5 BP	White	Polished	0	0	0	0	0	31,3
6 BPV	White	Polished + Glass	0	0	1	0	0	38,9
7 BPCV	White	Polished + Chamber + Glass	0	0	1	1	0	37,8
8 NN	Black	Rough	1	1	0	0	0	39,5
9 NNV	Black	Rough + Glass	1	1	1	0	0	44,9
10 NNCV	Black	Rough + Chamber + Glass	1	1	1	1	0	47,5
11 NCF	Black	Rough + Faceted	1	1	0	0	1	43,5
12 NP	Black	Polished	1	0	0	0	0	44,3
13 NPV	Black	Polished + Glass	1	0	1	0	0	49,0
14 NPCV	Black	Polished + Chamber + Glass	1	0	1	1	0	50,6

Table 1. Surface properties of the tested tiles and results of the irradiation tests.

In order to obtain more relevant information from the tests, the results were fitted to a mathematical model, whose characteristic parameters indicated how the different factors being studied affected the ΔT_{max} value. This mathematical model is given by the following equation:

$$\Delta T = b_1 X_1 + b_2 X_2 + b_3 X_3 + b_4 X_4 + b_5 X_5 + T_0$$

Equation 1

where b_i are the model fitting parameters; X_i are a series of Boolean variables, also given in Table 1, whose unit value indicates the presence of a specific property in a tile and whose zero value indicates that such a property is absent in the tile; and value T_o (°C) is the independent term of the fit. This model is useful in that the variables with a high related fitting parameter are those that have the greatest effect on radiation capture, while in contrast, those with the lowest fitting parameters have a less significant effect, which may even be detrimental when the fitting parameters are negative.

Variable	Effect on "ΔT" (b_i)
Colour (X_1)	10,4
Finish (X_2)	-2,1
Glass (X_3)	6,7
Chamber (X_4)	0,7
Faceted (X_5)	1,9

Table 2. Values of the fitting parameters.

Variable	Effect on "ΔT" without wind	Effect on "ΔT" with wind
Glass (X_3)	4,7	1,7
Spacer (X_4)	1,6	9,7

Table 3. Values of the fitting parameters under conditions with and without wind.

The fit of the experimental data in Table 1, using the least squares method, allowed the fitting parameters listed in Table 2 to be obtained.

The highest fitting parameter corresponded to the colour variable, which indicates that this factor has the greatest influence on radiation capture. Indeed, for the same surface finish, black tiles reached a significantly higher temperature than white tiles. The presence of glass on the tile surface is the second most important factor after tile colour. In fact, for the same tile surface characteristics, the placement of glass on the ceramic surface entails an increase in maximum temperature of between 5 and 9 °C.

Together with these tests conducted without wind, the study examined the effect of an air chamber between the ceramic tile and the glass placed on top, with the presence of wind. Table 3 gives the values of the fitting parameters that indicate the effect of the variables glass and air chamber on radiation capture in the presence and in the absence of wind. It may be observed that, when wind is present, the effect of the air chamber is much more significant than in the initial tests. This is because the air chamber minimises heat transfer by conduction from the tile towards the glass, reducing losses by convection to the ambient when wind is present.

2.3. DESIGN OF THE VENTILATED ENVELOPE PROTOTYPE

To study the performance of a ventilated ceramic envelope under real weather conditions, a prototype was designed and built, which is schematically illustrated in

Figure 4. This experimental assembly was built with a metal frame on which 60-mm-thick heat insulation panels were fixed. The prototype has an inner booth with access through one of the sides, which is divided into two chambers by means of an insulated partition (A). The rear part of the booth (B) houses part of the instrumentation, while the wall that forms the stabilisation sector (C) and the HTC (D) are located at the front. The width of the HTC can be adjusted depending on the needs of the experiment by moving the middle partition.

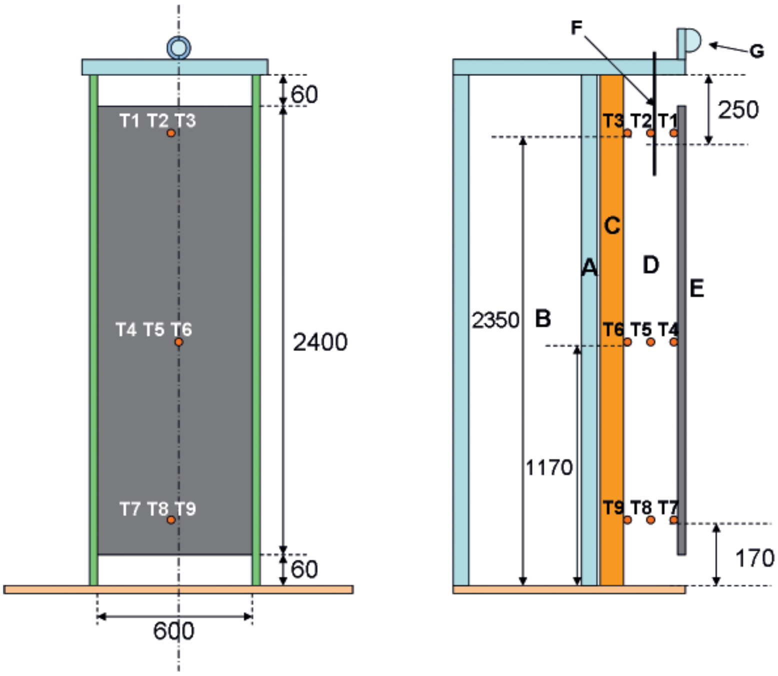

Figure 4. Schematic illustration of the experimental module.

The front of the booth is fitted with plastic side guides on which the tiles (E) that constitute the capturing elements of the envelope are fixed.

On the basis of the results obtained in the laboratory capture tests, the initially installed capture system consisted of two black porcelain tiles, 120x60 cm in size, which formed a capture area of 240x60 cm. Two 3-mm-thick glass sheets, of the same size as the tiles, were placed on top of the tiles, leaving a 3-mm gap.

Figure 4 also shows the position of the temperature sensors (J-type thermocouples). The thermocouples were fitted to record the temperature evolution in the part behind the capture area (T1, T4, and T7), of the air circulating through the HTC (T2, T5, and T8), and of the outer face of the stabilisation wall (T3, T6, and T9), all thermocouples being fitted at three different heights. Given the importance of heat transfer by radiation between the stabilisation wall and the inner surface of the capture sector, the thermocouples used to measure the surface temperature of these parts were set in small recesses, about 1 mm deep, which were covered with a putty made from a slurry of clay and ceramic pigments, in order to keep the radiation properties in the measurement area similar to those in the rest of the surface.

A Campbell LPO2 thermopile pyranometer (G) was fitted to the structure of the prototype to measure incident solar radiation (direct+diffuse) on the outer surface of the envelope. In order to measure this radiation accurately, the pyranometer needed to be fitted vertically, with the measuring plane parallel to the prototype capture surface. A Testo hotwire anemometer probe (F) was fitted at the top of the HTC to measure air speed inside the channel.

A heat exchanger was fitted between the stabilisation sector and the centre insulation in the prototype to measure the heat flow crossing the stabilisation module in the envelope. The heat exchanger consisted of a series of capillary tubes with an inner diameter of 3 mm, through which water was circulated at a constant temperature. In daytime working conditions, with the presence of solar radiation, as the water travelled through the exchanger it absorbed the heat from the wall, which increased the water temperature. In contrast, in the night-time functioning mode, or in the absence of solar radiation, when the ambient temperature was lower than the temperature of the incoming water, heat passed from the water to the wall, thereby lowering wall temperature. Knowing the difference between the water input and output temperatures (measured with two Pt100 heat resistances) and the circulation flow rate through the heat exchanger allowed determination of the heat flow density through the stabilisation sector at all times.

In addition to measurement of all the foregoing variables, ambient and wind temperature were also measured. All signals were collected by a Eurotherm data logger, which allowed data from all variables to be recorded every five minutes.

2.4. EXPOSURE UNDER ACTUAL CONDITIONS

Figure 5 shows a photograph of the prototype standing on the roof of the Instituto de Tecnología Cerámica (ITC). The assembly was arranged with the capture surface facing south, making sure that nearby building features projected no shadows on the assembly throughout the day at any time of year.

The evolution during a summer day of ambient temperature (T_{ex}), of the average temperature of the ceramic tile (T_p), of the air in the heat transfer channel (T_{am}), and of the outside surface of the stabilisation wall (T_{me}) has been plotted on the left axis in Figure 6. The evolution of the solar radiation impinging on the capture surface is plotted on the right axis. Figure 7 presents the evolution of these same variables for a day in winter.

Figure 5. Front view of the ventilated envelope prototype.

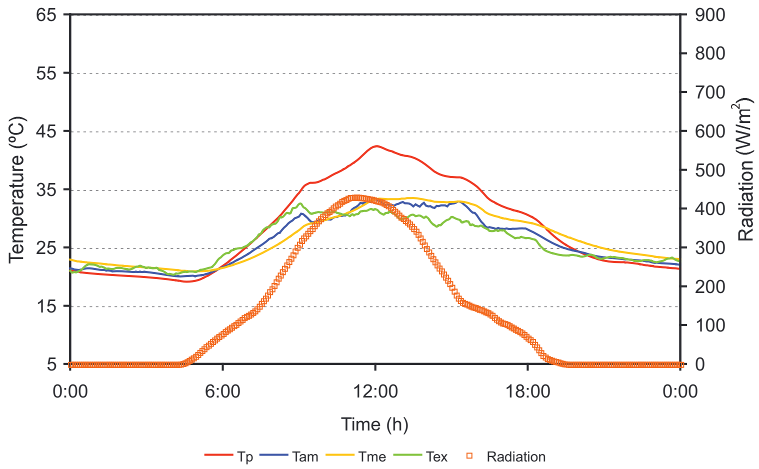

Figure 6. Evolution of some of the recorded variables on a summer day.

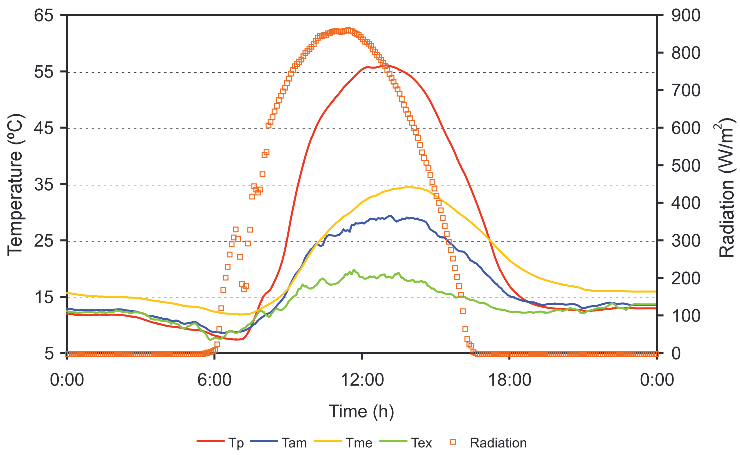

Figure 7. Evolution of some of the recorded variables on a winter day.

The main difference in prototype performance is observed to lie in the fact that the temperatures reached by the ceramic tile in winter (57 ºC at noon) are much higher than in summer (40 ºC at noon). This is because the incident radiation during winter is greater than in summer as a result of the lower angle of incidence of the solar radiation with respect to the surface of the Earth. Furthermore, given that the tile heats up more in winter, the air inside the HTC reaches temperatures at midday about 10ºC higher than ambient temperature, while in summer this difference is only 2 °C.

To estimate the energy performance of the envelope, its energy efficiency was calculated as the quotient of the energy transferred to the air circulating in the HTC, calculated from Equation 2, divided by the impinging solar energy.

$$E_a = mC_{pa}(T_{aL} - T_{ex})$$

Equation 2

It was verified that this calculation could not be used in point form, since the accumulation present in the system distorted the results, at times producing anomalous performance values. For this reason, in order to estimate the envelope's energy performance, it was necessary to work with the average energy values resulting from the integration of the entire day's incident radiation and energy use data

3. ANALYSIS OF HEAT TRANSFER PHENOMENA

In order to be able to evaluate the energy performance of the developed prototype, under different weather conditions and for different internal configurations, a mathematical model has been developed that is capable of accurately describing the prototype's thermal behaviour.

Figure 8 schematically illustrates the different heat transmission mechanisms involved in the proposed mathematical model. A one-dimensional model has been chosen, in which all heat exchanges only take place in the x direction.

The equations that model the behaviour of each envelope sector are described below.

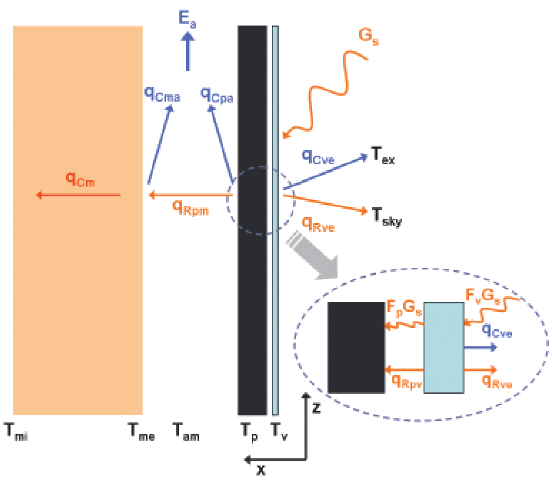

Figure 8. Heat exchange mechanisms.

3.1. MODELLING THE CAPTURE SYSTEM

The capture system has been modelled making the assumption that there is no energy accumulation in any of its components. For this reason, it has been assumed that the temperature of the glass and the temperature of the ceramic tile are uniform in the z direction and that heat transfer takes place in a quasi-steady state. In the characteristic equations posited for this sector, the glass sheet and the ceramic tile have been treated separately, and no heat exchange has been assumed to exist by convection or conduction inside the air chamber because, given its narrowness (3 mm), convection currents cannot be generated inside it and, since the thermal conductivity of air is very low, transport by conduction through it is negligible.

3.1.1. Glass sheet

The glass receives the impinging solar radiation, and it exchanges heat by convection with the atmosphere and by radiation with the atmosphere and the ceramic tile (see details in Figure 8). Equation 3 represents the energy balance in a quasi-steady state applied to the glass sheet [7]:

$$h_{Cve}(T_v - T_{ex}) + h_{Rve}(T_v - T_{sky}) + h_{Rvi}(T_v - T_p) - F_v G_s = 0$$

Equation 3

where h_{Cve} is the coefficient of heat transfer by convection between the glass and the outside ambient, which is related to wind speed [8], h_{Rve} is the coefficient of heat transmission by radiation between the glass and the sky [9], h_{Rvi} is the coefficient of heat transfer by radiation between the glass and the tile, and F_vG_s is the quantity of solar radiation absorbed by the glass [10].

3.1.2. Ceramic tile

The ceramic tile absorbs part of the solar radiation transmitted through the glass (α F_pG_s), and it exchanges heat by convection with the air present in the HTC and by radiation with the glass sheet and the outer surface of the stabilisation wall. Equation 4 constitutes the energy balance applied to the ceramic tile:

$$h_{Rpe}(T_p - T_v) + h_{Cp}(T_p - T_{am}) + h_{Rpi}(T_p - T_{me}) - \alpha F_p G_s = 0$$

Equation 4

where h_{Rpe} is the coefficient of heat transfer by radiation between the tile and the glass, h_{Rpi} is the coefficient of heat transfer by radiation between the tile and the inner face of the stabilisation wall, and h_{Cp} is the coefficient of heat exchange by convection between the tile and the air circulating through the HTC.

3.2. MODELLING THE HEAT TRANSFER CHANNEL

The modelling of the HTC was tackled from two points of view. On the one hand, the equations corresponding to the one-dimensional model schematically illustrated in Figure 8 were posited and solved and, on the other, the fluidodynamic behaviour of the HTC was modelled using a CFD (Computational Fluid Dynamic) code in order to determine the velocity and temperature profiles in the HTC. Modelling by CFD has served to verify that the assumptions made to solve the one-dimensional model were correct and to validate the velocity and temperature measuring points in the HTC.

3.2.1. Energy balances in the quasi-steady state applied to the HTC

It was experimentally verified that, given air's low heating capacity, the energy accumulation in the HTC was practically zero. Thus, application of a steady state energy balance to an infinitesimal section of the HTC of height dz, in which air is at temperature T_a, allows Equation 5 to be obtained, which relates average air temperature in the HTC, T_{am}, to both input temperature, T_{ao}, and output temperature, T_{aL}.

$$T_{am} = \phi T_{ao} + (1-\phi) T_{aL}$$

Equation 5

where $\phi = \frac{1}{\gamma L} - \frac{1}{e^{\gamma L} - 1}$ and $\gamma = b(h_{Cme} + h_{Cp})/(mC_{pa})$. The calculation of T_{am} implies knowing the direction of the air flow inside the channel, since T_{ao} and T_{aL} adopt different values depending on whether the air flow, m, is upward or downward. Application of a mechanical energy balance to the HTC yields Equation 6 with which, once the value of the coefficient of discharge $K^{1/2}$ has been experimentally obtained, the mass flow rate of the air circulating in the HTC can be calculated as a function of T_{am} and the outside air temperature, T_{ex}.

$$m = \frac{\rho_{am} A_c}{\sqrt{K}} \sqrt{\frac{2gL(T_{am} - T_{ex})}{T_{ex}}}$$

Equation 6

3.2.2. CFD modelling: velocity and temperature profiles in the HTC

The thermal and fluidodynamic behaviour of the envelope has been simulated using the ANSYS-CFX v10 CFD (Computational Fluid Dynamic) code, using a 2D model that represents an axial cross-section of the envelope situated on its vertical symmetry plane. The only simplification made in this simulation was the elimination of the glass sheet from the capture sector. The effect produced by this glass sheet was obtained by a variation of the coefficient of heat transmission by convection between the outside air and the glass sheet.

The meshing of the model combines structure mesh together with the surfaces (in order to improve processing of the fluido–structure interaction) and non-structured mesh in the fluid (for improved refining in the difficult areas and node economy). On average, the computational region representing the radiation capture sector is represented by about 7,000 nodes, while the region simulating the fluid contained in the HTC is divided into 43,000 nodes. Figure 9 shows an example of the meshing of the top of the HTC.

A two-equation turbulence model, the *Shear Stress Transport* model, was chosen. It is very important that the prediction should be accurate near the walls, since the natural convection mechanism is based on this phenomenon. Special processing was chosen, applying a *Gamma Theta* model for turbulence transition. In order to model the heat transmission by radiation in the HTC, a model based on Monte Carlo techniques was chosen.

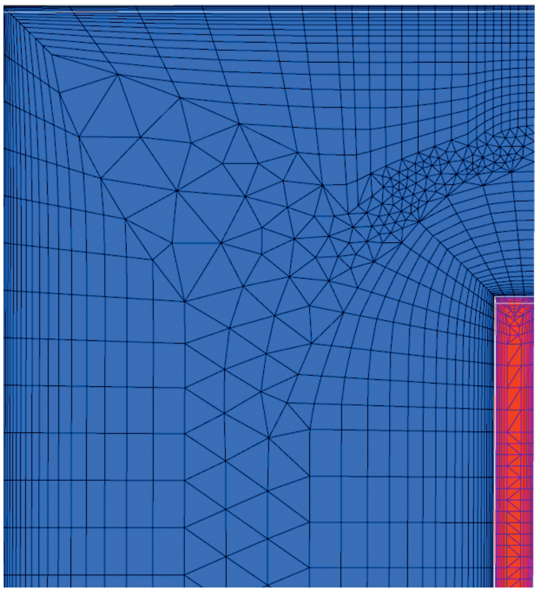

Figure 9. Example of meshing at the top of the HTC.

Figure 10 shows examples of temperature and velocity distributions at the top and bottom of the HTC obtained using these simulations.

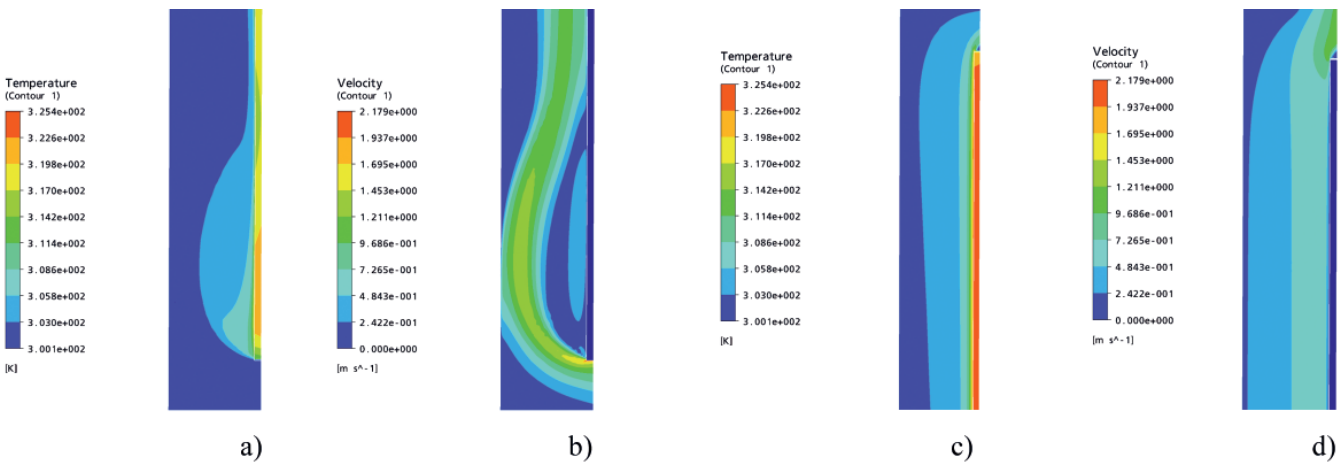

Figure 10. Temperature and velocity distributions obtained with incident radiation of 500 W/m² and outside temperature of 27 °C: a) and b) bottom of HTC; c) and d) top of HTC.

3.3. MODELLING OF THE STABILISATION SECTOR

The equation used for the non-steady energy balance applied to the stabilisation wall has the following form:

$$\frac{\partial T}{\partial t} = \alpha \frac{\partial^2 T}{\partial x^2}$$

Equation 7

To solve Equation 7, a numerical method based on the Cranck-Nicholson discretisation scheme was used, setting the temperature inside the wall and the heat flow at the outer surface of the wall as boundary conditions.

3.4. VALIDATION OF THE PROPOSED MODEL

The equations that describe the behaviour of each envelope sector were implemented in a calculation program developed with *Scilab* open code software [11]. The data of the incident solar radiation, ambient temperature, wind speed, and temperature of the inner surface of the stabilisation wall were used to model the behaviour of the prototype for several typical days.

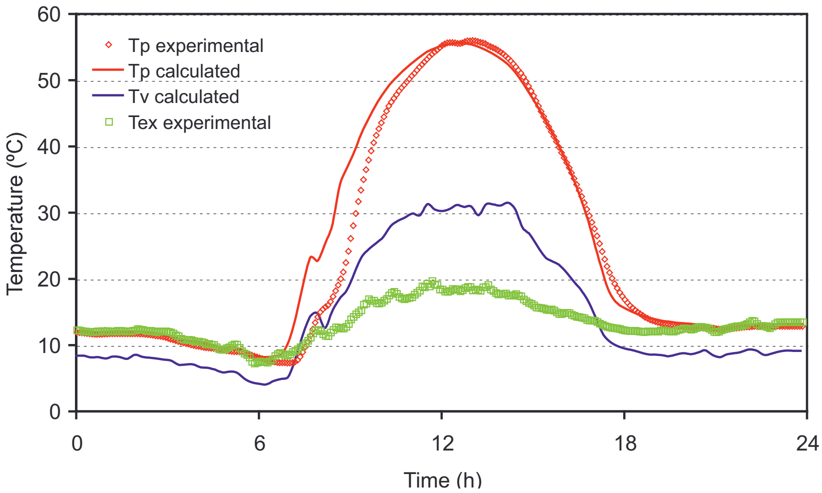

Figure 11. Evolution of tile temperature and glass temperature.

The evolution of tile temperature predicted by the model and of tile temperature recorded experimentally, for the same day as the data given in Figure 7, is displayed in Figure 11. The figure also shows the evolution of glass temperature calculated from the model and experimental ambient temperature. It may be observed that the tile temperature curve calculated from the model fits the experimental data quite well. The slight difference between the curves may be due to the fact that the model does not consider the energy accumulation that might exist in the capture sector. During the night, the glass temperature is lower than the ambient temperature owing to the heat that the glass loses to the atmosphere through radiation.

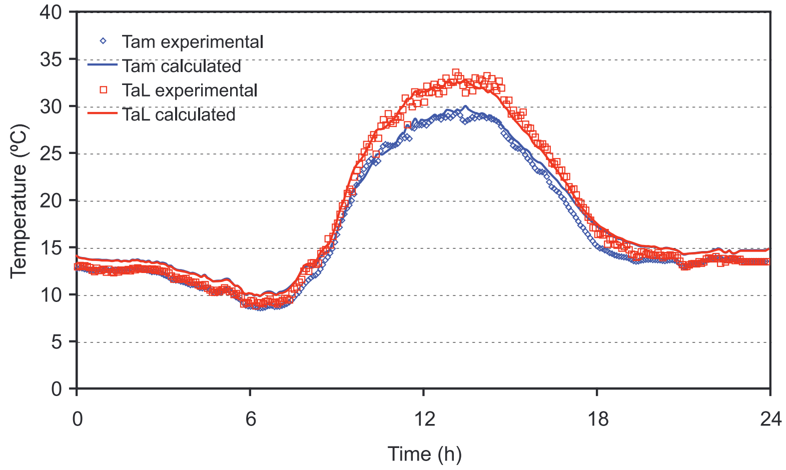

Figure 12. Evolution of average air temperature inside the HTC and the output aire temperature.

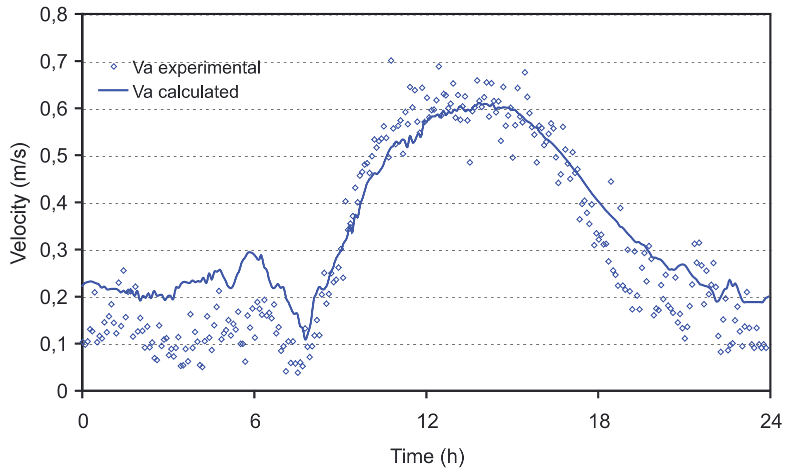

Figure 13. Evolution of aire speed.

The evolution of average air temperature inside the HTC and output air temperature, both calculated from the model, have been plotted for the same day in Figure 12. The fit with the experimental data is observed to be acceptable, which validates the assumptions made in positing the model for the HTC. Finally, the evolution of air speed inside the HTC, calculated from the model as an absolute value, and the experimental air speed, recorded with the hot wire anemometer on the prototype, have been plotted in Figure 13. The experimental data are observed to acceptably fit the values predicted by the model.

4. CONCLUSIONS

- A system has been built to reproduce irradiation conditions in the laboratory similar to solar radiation conditions, which allows the radiant-energy absorption capacity of ceramic tiles intended for ventilated building envelopes to be studied.
- The influence of the surface properties of these ceramic tiles on their behaviour in relation to solar radiation has been studied.

- A prototype has been designed and built to study the energy performance of ventilated ceramic envelopes under actual exposure conditions.
- The experimental data obtained from the prototype have been used to develop and validate a mathematical model that describes the thermal behaviour of ventilated ceramic envelopes.

REFERENCES

[1] Código Técnico de la Edificación. http://www.codigotecnico.org [Consulta: 2007-09-25]

[2] L. ZALEWSKI et al. Experimental thermal study of a solar wall of composite type. *Energy Build.* 25, 7-18, 1997.

[3] J. MARTÍ-HERRERO, M.R. HERAS-CELEMIN. Dynamic physical model for a solar chimney. *Sol. Energy* 81, 614-622, 2007.

[4] J. SHEN et al. Numerical study on thermal behavior of classical or composite trombe solar walls. *Energy Build.*, 39 (8), 962-974, 2007.

[5] M. CIAMPI, F. LECCESE, G. TUONI. Ventilated facades energy performance in summer cooling of buildings. *Sol. Energy* 75, 491-502, 2003.

[6] J. RAYMOND, E. BILGEN. On the thermal and ventilation performance of composite walls. *Energy Build.* 9 (39), 1041-1046, 2006.

[7] F. P. INCROPERA, D. P. DE WITT. *Fundamentals of heat and mass transfer*. 3rd ed. Chichester: John Wiley & Sons, 1990.

[8] W. H. McADAMS. *Heat transmission*. 3rd ed . New York: McGraw-Hill, 1994.

[9] L. ADELARD et al. Sky temperature modelisation and applications in building simulation. *Renew. Energy* 15, 418-430, 1998.

[10] M. F. MODEST. *Radiative heat transfer*. New York: McGraw-Hill, 1993.

[11] Scilab Home Page. http://www.scilab.org [Consulta: 2007-09-20]

NOMENCLATURE

T_v: glass temperature (ºC)

T_p: ceramic tile temperature (ºC)

T_{am}: average air temperature in the HTC (ºC)

T_{ao}: input air temperature in the HTC (ºC)

T_{aL}: output air temperature of the HTC (ºC)

T_{me}: outside temperature of the stabilisation wall (ºC)

T_{mi}: inside temperature of the stabilisation wall (ºC)

T_{ex}: outside ambient temperature (ºC)

T_{sky}: sky temperature (ºC)

G_s: solar radiation (W/m^2)

E_a: energy transferred to air in the HTC (W)

q_R: density of heat flow by radiation (W/m^2)

q_C: density of heat flow by conduction or convection (W/m^2)

F_p: radiation fraction absorbed by the tile

F_v: radiation fraction absorbed by the glass

h_C: coefficient of heat exchange by convection (W/(m^2 K))

h_R: coefficient of heat exchange by radiation (W/(m^2 K))

b: HTC width (m)

L: HTC height (m)

A_c: HTC pass cross-section (m^2)

m: mass flow rate of the air circulating through the HTC (kg/s)

C_{pa}: specific heat of air (J/(kg K))

ρ_a: density of air (kg/m^3)

g: gravity acceleration (m/s^2)

K: HTC coefficient of discharge

α: thermal diffusivity of the stabilisation wall (m^2/s)

ACKNOWLEDGEMENTS

The study presented is the result of a research project co-financed by the Spanish Ministry of Development [National Plan for R&D&I 2004/2007 – National Programme for Construction of the Transport Area and Construction (2004/60)], and the Spanish Ministry of Industry, Tourism, and Trade [National Plan for Scientific Research, Development and Technological Innovation 2004-2007 – Programme for Fostering Technical Research– FIT 380000-2005-159].